BLOOD SHEAR STRESS IN A CHICKEN EMBRYO, EXPERIMENTS AND NUMERICAL MODELING

Mathieu Pourquie, Peter Vennemann, J. Westerweel, R. Lindken
Lab for Aero- and hydrodynamics
Delft University of technology
Delft
Netherlands
m.j.b.m.pourquie@wbmt.tudelft.nl

B. Hierck, B. Groenendijk, R. Poelmann
Department of Anatomy and Embryology
Leiden University Medical Center
Leiden
Netherlands

S. Stekelenburg-DeVos, N. Ursem
Department of Obstetrics and Gynecology
Erasmus MC
Rotterdam
Netherlands

ABSTRACT

There is evidence that there is a connection between the shear stress distribution at the wall of the developing, embryonic heart and growth errors. This relationship needs to be verified and quantified using experiments and a numerical model. The chicken embryo is a perfect model to investigate these aspects because of its size and because it is easily accessible.

GEOMETRY OVERVIEW

The geometry studied is shown in Figure 1. The chicken embryo is shown with head, eye, and developing spine visible. The heart (indicated by H in the figure) has the form of a curved tube in this stage of growth. It is visible because of the blood flowing through. Part of the vessel system in the egg yolk is also shown. The heart diameter is about 0.1 mm, the length 0.3 mm and the Reynolds number is of the order 1. The form of the curved tube becomes more complicated during its development.

EXPERIMENTS

Gene expressions

Some genes have been shown to be shear stress responsive. These include genes for proteins that regulate blood vessel function, like endothelin (ET1) and nitric oxide synthase (NOS3), and genes that regulate other genes, i.e. transcription factors like Kruppel-like factor (KLF2). The presence of these genes was determined in the chicken heart, and was used to delineate the shear stress patterns and the biological response to those patterns. See Figure 2 which shows the lumen together with KLF2 indication (reconstructed from 2D planes) for the heart and surrounding vessels. The KLF2 indication marks parts of the vessel wall with high shear stress. The figure is rotated 180 degrees with respect to Figure 1. The heart is the thick tube below. The thick tube is contracted at the position of the valves.

Changing blood flow through the embryo, by means of experimentally clipping one of the vitelline vessels that run to the heart, leads to immediate changes in heart function (Stekelenburg, 2003, 2005; Ursem, 2004), and to abnormal gene expression (Groenendijk et al., subm). This change in gene expression is considered to be the trigger for the congenital malformations (Hogers, 1997).

PV loops

Ventricular pressure-volume (PV) loops were obtained by means of simultaneous recording of (i) ventricular volume by video microscopy and (ii) intra-ventricular pressure by servo-null pressure measurement. These PV-loops demonstrated changes in myocardial function of the ventricles after obstruction of one of the vitelline veins (Figure 3, from Stekelenburg-De Vos, 2005). Simultaneous measurement of dorsal aortic volume flow and atrioventricular (AV) blood flow velocity provide information on passive and active cardiac filling volumes. This study demonstrated that ventricular filling is altered probably caused by a stiffer ventricle after venous obstruction (Ursem, 2004).

μPIV measurements

To investigate whether the gene expression patterns (Figure

2) are directly related to an abnormal shear stress distribution, the blood velocity distribution within the heart needs to be investigated. Therefore a μPIV (Micro Particle Image Velocimetry) system has been developed (Vennemann, 2005). Fluorescent liposomes with a nominal diameter of 400 nm are added to the flow as tracer. Because of their small dimension, the neutrally buoyant liposomes closely follow the movement of the blood plasma and allow the determination of the velocity gradient near the wall. Figure 4 shows the result of a μPIV measurement in the developing ventricle. A sample velocity profile has been extracted from the flow field and is being superimposed on the vector field as a continuous curve. The profile was an ensemble average over multiple heart-beats. The profile clearly shows an asymmetrical velocity distribution which suggests the highest shear stresses will appear at the inner curvature. Accordingly, a high level of gene expression can be found at the same location (Figure 2, inner curvature of the ventricle lumen).

CFD

The numerical model uses a 3D simulation of the embryonic heart geometry, for which we took curved tubes of various complexity. See Figure (5) which shows the wall shear stress pattern during motion of a typical geometry. In this case, most shear is present near the cushions. The model applies a prescribed motion during contraction and the heart is modelled as an elastic shell during the filling stage. Two ways of simulating the heart are considered. One uses a standard 3D unstructured collocated commercial package (Fluent) as described in for instance (Ferziger, 2003), with a moving grid. The other uses a so-called virtual boundary method on a staggered Cartesian grid. The virtual boundary is implemented by adding extra source terms to the N-S equations which push the fluid velocity to the correct value at the heart wall. See figure 7. The heart wall is represented by a triangulated surface. A related method has been used by Peskin et al (see Kovacs, 2003). Two models are considered instead of one for validation purposes, since the accuracy of virtual boundary methods for the prediction of shear stress needs to be assessed.

CFD results

As to the calculation of the wall stress, we have compared both models for entry flow in a straight, round pipe for $Re = 10$. The result is shown in the next figures (9 and 10). Both figures show some scatter about the true value (which becomes visible by adapting the contour levels). This scatter is the consequence of using a representation of a cylinder with triangles. The average value of the stress is 10 % lower, partly due to the way the inflow in the pipe was done. This indicates that the virtual boundary method is capable of predicting wall shear stress.

The simulation of the actual geometry has difficulties of its own, apart from the numerical treatment. The form of the heart is not exactly known. Also the manner in which it deforms is not always totally clear. It changes from peristaltic to beating during growth. A simplifying fact is that the Re number is quite low, it is of the order of 1. Moreover, measurements of the viscosity indicated a lower Non-Newtonian behavior than in adult blood. Summarizing, for the moment, qualitative agreement between the various methods is all we expect and studying model geometries which are simpler than the original model is worthwhile.

A simpler geometry is the one shown in figure 6 which shows the wall shear stress in a stationary geometry, consisting of a curved by with two end pipes. Highest shear (lighter parts) are shown near the inner curvature.

The stress distribution as found by two CFD models suggests a high shear stress near the position of the cushions. The inner part of the curved boundary has a higher shear stress than the outer part. This is qualitatively the same as for the KLF expression and is as good as we can compare at this moment.

CONCLUSION AND FURTHER WORK

The experimental data combined with the two numerical approaches result in a big quantity of data which can be compared (velocity profiles, PV loops, gene expression etc). So far qualitative agreement has been found. More results can be shown on the conference. Plans for the near future include more refined modeling of blood and heart-vessel walls. Moreover, for a proper description of the flow in the heart we need appropriate boundary conditions. These can be provided by a 1-D model for the artery-vein system (see Figure 8), which is coupled to the 3D heart, as described in (Smith, 2002). The 1D model can be coupled to the 3D model if the flow leaving the 3D part of the calculation domain is sufficiently developed and a 1D approximation applies. By adding some pieces of artery to the 3D part we can study the effect of clipping of vessels.

REFERENCES

Ferziger J and Peric M., Computational methods for fluid dynamics, Springer. 2002.

Groenendijk BCW, Hierck BP, Gittenberger-de Groot AC, Poelmann RE.,2004, "Development-related changes in the expression of shear stress responsive genes KLF-2, ET-1, and NOS-3 in the developing cardiovascular system of chicken embryos.", *Dev Dyn.*, 230 pp 57-68

Hogers B, DeRuiter MC, Gittenberger-de Groot AC, Poelmann RE.,1997, "Unilateral vitelline vein ligation alters intracardiac blood flow patterns and morphogenesis in the chick embryo." *Circ Res.* 80 pp 473-481.

Lindken R., Vennemann P., Westerweel, J., Ursem, NTC., Stekelenburg-de Vos, S., Poelman, R. , 2003, "In-vivo micro-PIV measurements in the embryonic avian heart." *Bulletin of the American Physical Society, Proc. of the 56th Annual Meeting of the Division of Fluid Mechanics*, session ME, biofluid dynamics VII,

Kovacs S. J., McQueen D. M., and Peskin C. S. , Modelling cardiac fluid dynamics and diastolic function, *Philos. Trans R Soc (A)* 359 pp 1299-1314, 2001.

Maenner, J., 2000. Cardiac looping in the chick embryo: A morphological review with special reference to terminological and biomechanical aspects of the looping process. *The Anatomical Record* 259, 248-262.

Smith N. P., Pullan A. J., and Hunter P. J., 2002, An anatomically based model of transient coronary blood flow in the heart , *SIAM J Appl Math* 62, pp 990-1018.

Stekelenburg-de Vos S, Steendijk P, Ursem NT, Wladimiroff JW, Delfos R, Poelmann RE., 2005, "Systolic and diastolic ventricular function assessed by pressure-volume

loops in the stage 21 venous clipped chick embryo." *Pediatric Research* , 57(1) pp 16-21

Stekelenburg-de Vos S, Ursem NT, Hop WC, Wladimiroff JW, Gittenberger-de Groot AC, Poelmann RE.,2003, "Acutely altered hemodynamics following venous obstruction in the early chick embryo." *Journal of x perimental Biology*, 206(Pt 6) pp1051-7

Ursem NT, Stekelenburg-de Vos S, Wladimiroff JW, Poelmann RE, Gittenberger-de Groot AC, Hu N, Clark EB.,2004, "Ventricular diastolic filling characteristics in stage-24 chick embryos after extra-embryonic venous obstruction." *Journal of x perimental Biology* 207(Pt 9) pp 1487-90

Vennemann, P., Kiger, K.T., Lindken R., Groenendijk, B. C. W., Stekelenburg-de Vos, S., ten Hagen, T. L. M., Ursem, N. T. C., Poelmann, R. E., Westerweel, J., Hierck, B. P., 2005. In vivo micro particle image velocimetry measurements of blood-plasma in the embryonic avian heart. Accepted for publication in: *Journal of Biomechanics.*

FIGURES

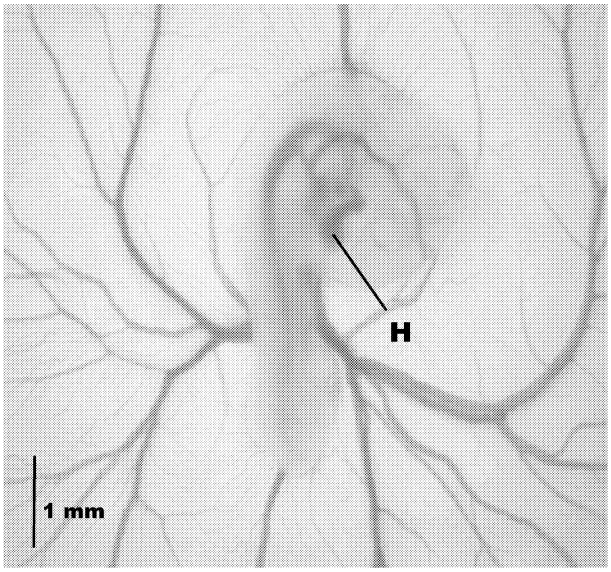

Figure 1: The chicken embryo together with the blood vessel system surrounding it. The heart is indicated by H).

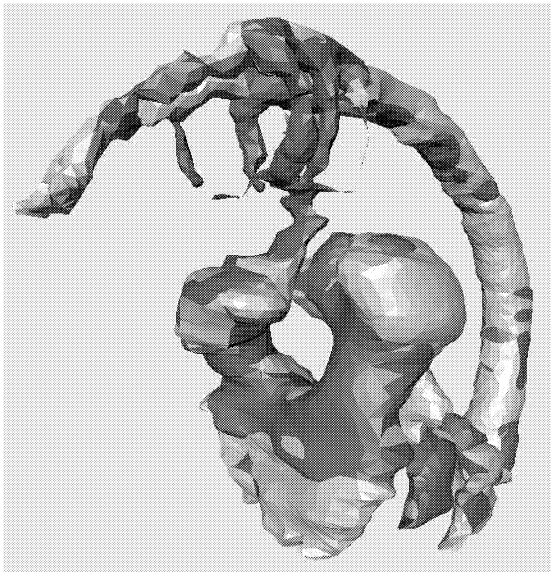

Figure 2: Lumen of the chicken embryo s heart (and some surrounding vessels). The dark parts indicate places where (high) shear is detected. From Groenendijk et al, 2004.

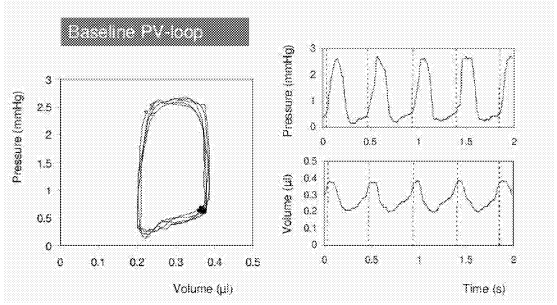

Figure 3: Measured PV loops (left) and P (upper right) and V (upper right) signals in time for the embryonic chicken heart.

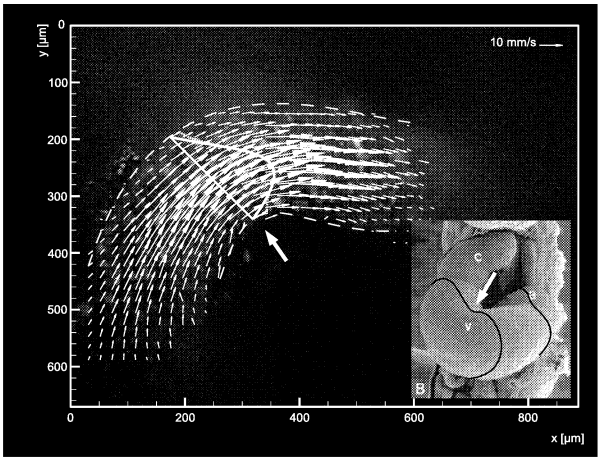

Figure 4: Velocity distributions in the developing ventricle (10x magnification) of a Stage 15 chicken embryo. A representative profile depicting the local ensemble-averaged, axis-normal velocity magnitude is superimposed on the vector field. The approximate lumen boundary is indicated by two dashed lines that are readily determined by interpolating the velocity profiles to zero. The location and spatial orientation of the measurement planes relative to the looping heart are indicated in the scanning electron micrographs from Mnner (2000).

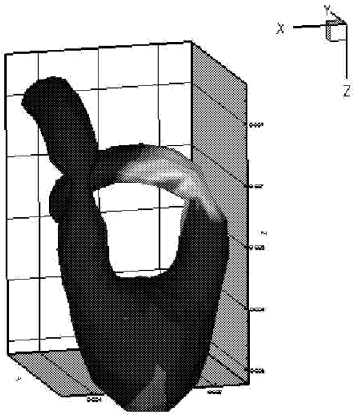

Figure 5: The geometrical form of an embryonic heart, colored by wall shear stress, light corresponds to high shear.

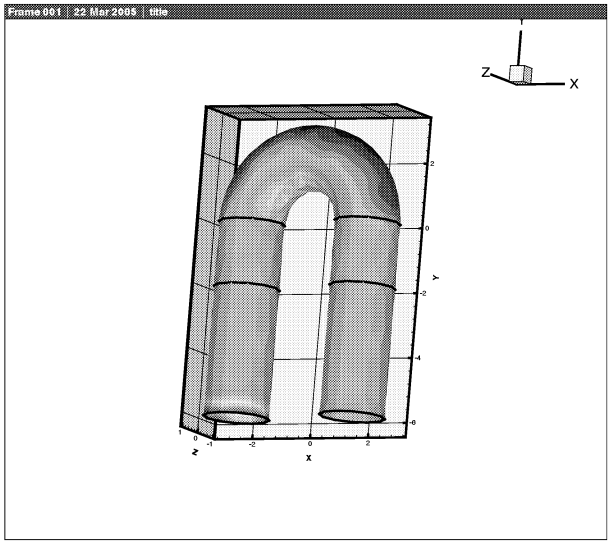

Figure 6: Shear stress distribution in a simpler geometry consisting of a curved pipe with two straight end pipes. Inflow from the left bottom, outflow at the right bottom. Light color indicates high wall shear stress, dark color indicates low wall shear stress.

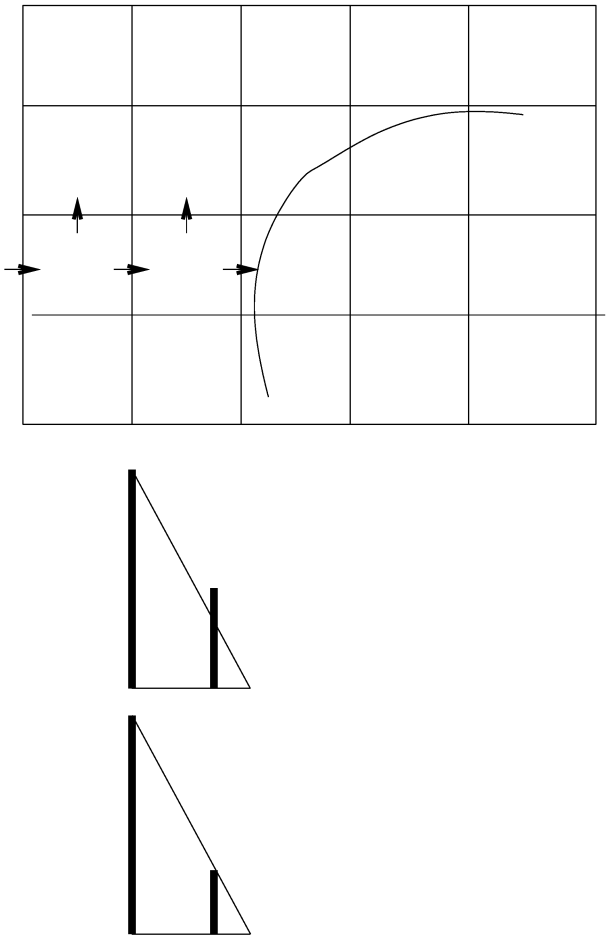

Figure 7: The Cartesian method explained. Velocities near the (curved) boundary are adapted such that linear interpolation of velocities near the boundary have the right magnitude.

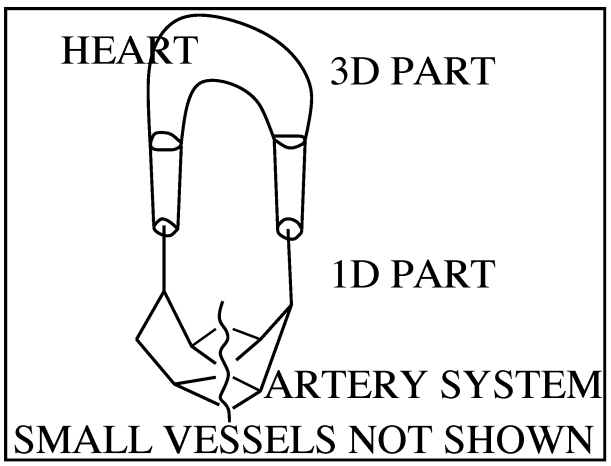

Figure 8: The complete circulation system. The figure indicates parts modeled 3D and parts modeled 1D.

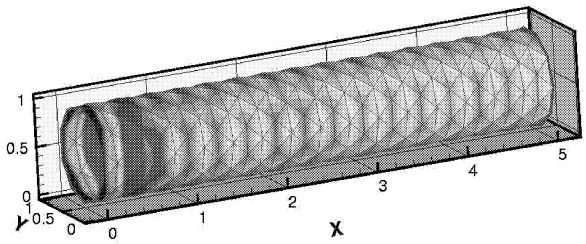

Figure 9: Shear stress contour plot for the Cartesian model, showing fluctuation due to triangularization of the surface.

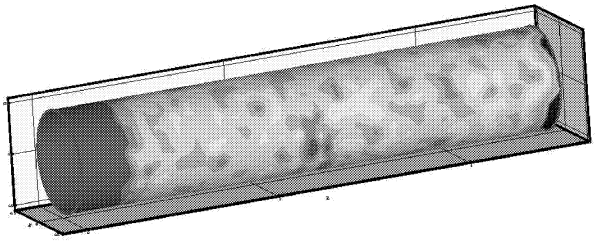

Figure 10: Shear stress contour plot for the unstructured model, showing fluctuation due to triangularization of the surface.